Report

Current Biology

Extreme Enlargement of the Cerebellum in a Clade of Teleost Fishes that Evolved a Novel Active Sensory System

Highlights

- Brains and brain regions vary widely in size and shape across osteoglossomorph fishes
- Extreme encephalization resulted from a concerted enlargement of all brain regions
- Active electrosensing evolved alongside an enlarged cerebellum and hindbrain
- Changes in brain structure may relate to the evolution of behavioral novelty

Authors

Kimberley V. Sukhum, Jerry Shen, Bruce A. Carlson

Correspondence

carlson.bruce@wustl.edu

In Brief

Sukhum et al. show that evolution of enlarged brains in osteoglossomorph fishes is associated with concerted increases in the sizes of all brain regions, but that active electrosensing evolved alongside independent changes in the sizes of different brain regions. Changes in brain structure may be most likely with the evolution of novel behaviors.

Sukhum et al., 2018, Current Biology *28*, 1–7
December 3, 2018
https://doi.org/10.1016/j.cub.2018.10.038

CellPress

Please cite this article in press as: Sukhum et al., Extreme Enlargement of the Cerebellum in a Clade of Teleost Fishes that Evolved a Novel Active Sensory System, Current Biology (2018), https://doi.org/10.1016/j.cub.2018.10.038

Current Biology
Report

Extreme Enlargement of the Cerebellum in a Clade of Teleost Fishes that Evolved a Novel Active Sensory System

Kimberley V. Sukhum,[1] Jerry Shen,[1] and Bruce A. Carlson[1,2,*]
[1]Department of Biology, Washington University in St. Louis, 1 Brookings Drive, St. Louis, MO 63130, USA
[2]Lead Contact
*Correspondence: carlson.bruce@wustl.edu
https://doi.org/10.1016/j.cub.2018.10.038

SUMMARY

Brains, and the distinct regions that make up brains, vary widely in size across vertebrates [1, 2]. Two prominent hypotheses have been proposed to explain brain region scaling evolution. The mosaic hypothesis proposes that changes in the relative sizes of particular brain regions are the result of selection acting independently on those regions [2, 3]. The concerted hypothesis proposes that the brain evolves as a coordinated structure due to developmental constraints [4]. These hypotheses have been widely debated [3–7], and recent studies suggest a combination of the two best describes vertebrate brain region scaling [8–10]. However, no study has addressed how the mosaic and concerted models relate to the evolution of novel behavioral phenotypes. We addressed this question using African mormyroid fishes. The mormyroids have evolved a novel active electrosensory system and are well known for having extreme encephalization [11] and a large cerebellum [2, 12], which is cited as a possible example of mosaic evolution [2]. We found that compared to outgroups without active electrosensing, mormyroids experienced mosaic increases in the sizes of the cerebellum and hindbrain, and mosaic decreases in the sizes of the telencephalon, optic tectum, and olfactory bulb. However, the evolution of extreme encephalization within mormyroids was associated with concerted changes in the sizes of all brain regions. This suggests that mosaic evolutionary change in the regional composition of the brain is most likely to occur alongside the evolution of novel behavioral functions, but not with the evolution of extreme encephalization.

RESULTS

The Cerebellum Is Enlarged in Mormyroid Species

Passive electrosensing via ampullary electroreceptors evolved first in osteoglossomorph fishes, allowing for the detection of external bioelectric fields [13]. Active electrolocation and communication then arose with the evolution of electric organs and tuberous electroreceptors in mormyroids [13]. Brain regions involved in generating and processing electric signals were most likely subject to strong and consistent selection compared to other brain regions, providing an excellent system to test for mosaic evolution.

We studied two outgroup species with no electrosensory system (*Pantodon buchholzi* and *Chitala ornata*), one outgroup species with passive electrosensing (*Xenomystus nigri*), the sole active electrosensing mormyroid species in a sister clade to the family Mormyridae (*Gymnarchus niloticus*), and six mormyrid species (Figure 1A). The six mormyrids represent the greatest variation in phylogenetic relatedness and relative brain size across mormyrids: *Campylomormyrus* spp., *Gnathonemus petersii*, and *Mormyrus tapirus* have high encephalization, *Brevimyrus niger* and *Petrocephalus tenuicauda* have intermediate encephalization, and *Brienomyrus brachyistius* has low encephalization [11].

To determine how brain region size varies across species, we compared 3D reconstructions of brains that were divided into six homologous regions: telencephalon (TEL), olfactory bulb (OB), optic tectum (OT), cerebellum (CB), hindbrain (HB), and the rest of the brain (RoB) (Figure 1B; Video S1). The rest of the brain included hypothalamus, thalamus, and midbrain regions other than OT (see STAR Methods). We found that the cerebellum is enlarged in mormyrids compared to outgroup species, with the mormyroid *G. niloticus* having an intermediate cerebellum (Figure 1B). In large-brained mormyrids, the cerebellum appears to constitute an even larger proportion of the brain, extending further over hindbrain and telencephalon than in small-brained species (Figure 1B).

Mosaic Shifts in Brain Region Sizes Occurred in the Common Ancestor of Mormyroids

To compare brain region size relative to total brain size, we measured the volume of each region and modeled brain region scaling by performing phylogenetic generalized least squares (PGLS). Within mormyroids and among the outgroups, each brain region correlated positively with total brain size (Figure 2).

We performed an analysis of covariance (ANCOVA) that compared mormyroids to outgroups using the PGLS relationships of brain region volume against total brain volume (Table S1). We found a grade shift among different brain regions between mormyroids and outgroups (Figures 2A–2E). For cerebellum and hindbrain, mormyroids had a larger y intercept than outgroups,

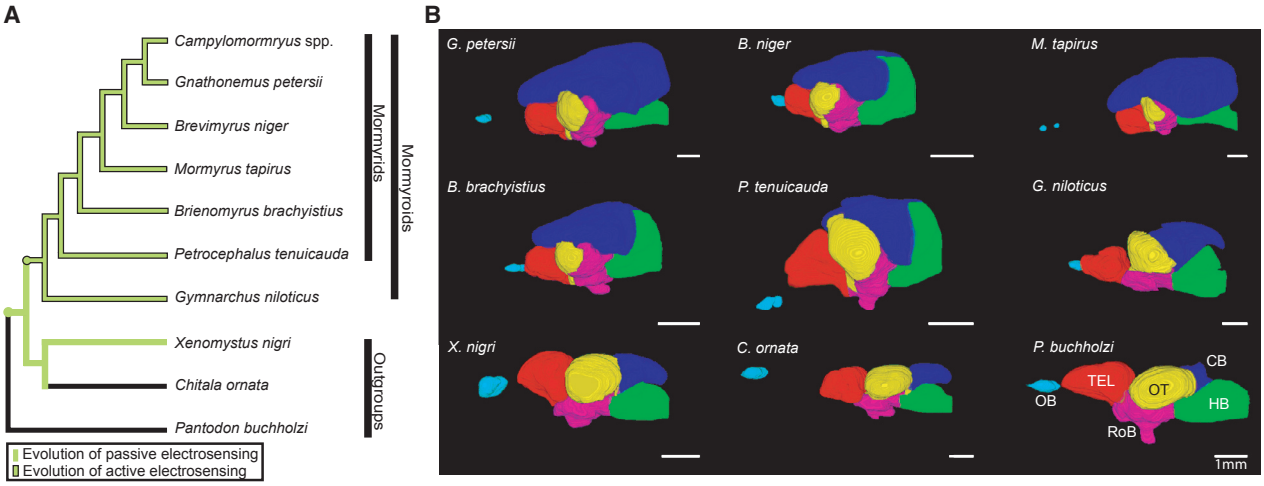

Figure 1. Brain Region Variation across Osteoglossomorphs

(A) Cladogram based on consensus trees [14–16] of the species studied. Green indicates the evolution of passive electrosensing [16]. Black outline indicates the evolution of active electrosensing [16].

(B) 3D reconstructions from micro-computed tomography scans show expansion of the cerebellum in mormyroids. Brains were oriented from a lateral view with posterior to the right and dorsal on top. Colors indicate corresponding regions for each brain: telencephalon (TEL; red), cerebellum (CB; dark blue), optic tectum (OT; yellow), olfactory bulb (OB; light blue), hindbrain (HB; green), and rest of brain (RoB; magenta).

See also Video S1.

indicating an increase in cerebellum and hindbrain that was independent of total brain size ($p_{CB} < 10^{-12}$; $p_{HB} < 0.01$; Figures 2A and 2E). For telencephalon, olfactory bulbs, and optic tectum, the outgroup species had a larger y intercept ($p_{TEL} < 10^{-6}$; $p_{OB} < 10^{-8}$; $p_{OT} < 10^{-13}$; Figures 2B–2D). There was no significant difference in y intercept between the two grades in the rest of the brain ($p_{RoB} = 0.217$; Figure 2F). Therefore, significant shifts in relative brain region sizes occurred in the most recent common ancestor of mormyroids.

To determine whether mosaic shifts evolved in taxa that evolved passive, but not active, electrosensing, we ran an ANCOVA between *X. nigri* and *C. ornata* (Table S1). *X. nigri* had a larger y intercept than *C. ornata* for telencephalon and a smaller y intercept for cerebellum and the rest of the brain ($p_{TEL} < 10^{-4}$; $p_{CB} < 0.05$; $p_{ROB} < 10^{-5}$; Figure 2). These results reveal that there are mosaic shifts between these species, but in different directions from those that occurred in mormyroid evolution.

To determine whether mosaic shifts co-occurred with the evolution of extreme encephalization, as suggested in primates [4], we ran an ANCOVA that corrected for phylogenetic relatedness on mormyrid species with large brains against mormyrids with intermediate to small brains (Table S1). This revealed similar relationships for each region except the olfactory bulbs (Figure 2), for which large-brained species had a smaller y intercept ($p < 10^{-3}$). This suggests that as total relative brain size increased in mormyrids, brain regions primarily scaled concertedly.

Given debate over the best way to quantify brain region scaling [4, 6], we also compared each region against every other region (Figure S1), and each region against total brain size minus the respective brain region (Figure S2). Both methods showed a grade shift between mormyroid and outgroup species for cerebellum, hindbrain, telencephalon, optic tectum, and olfactory bulb, demonstrating that the grade shift associated with the evolution of mormyroids is not dependent on a particular method of comparison.

Both Concerted and Mosaic Evolution Are Evident across Osteoglossomorphs

To better understand coordinated variation in brain region sizes, we ran a phylogenetic principal component analysis (PCA). We used the species mean volumes of each region in a PCA to determine the rotational axis, and then we calculated individual scores for each specimen. PC1 explained 85.31% of the variation among all species. All brain regions loaded positively on PC1, and this axis was strongly correlated with total brain size (slope, 2.16; intercept, −3.85; $p < 10^{-15}$; $r^2 = 0.986$) (Figure 3). These data support the concerted hypothesis and demonstrate that most variation in brain region size is highly correlated with total brain size.

Interestingly, total brain size did not account for all variation. For PC2, olfactory bulb, telencephalon, and optic tectum loaded negatively, whereas cerebellum and hindbrain loaded positively (Figure 3). PC2 illustrates mosaic shifts in brain regions that separated mormyroids from outgroups, and this component accounted for 12.45% of total variation in volume size (Figure 3). These data demonstrate that there is a component of variation in brain region sizes that does not scale with total brain size but instead separates mormyroids from outgroups. There was, however, no separation between the passive electrosensing *X. nigri* and other outgroup species.

To a lesser extent, PC1 and PC2 separated mormyrid species with high encephalization from species with intermediate to low encephalization (Figure 3). Because a grade shift between encephalization degree within mormyrids was only found in

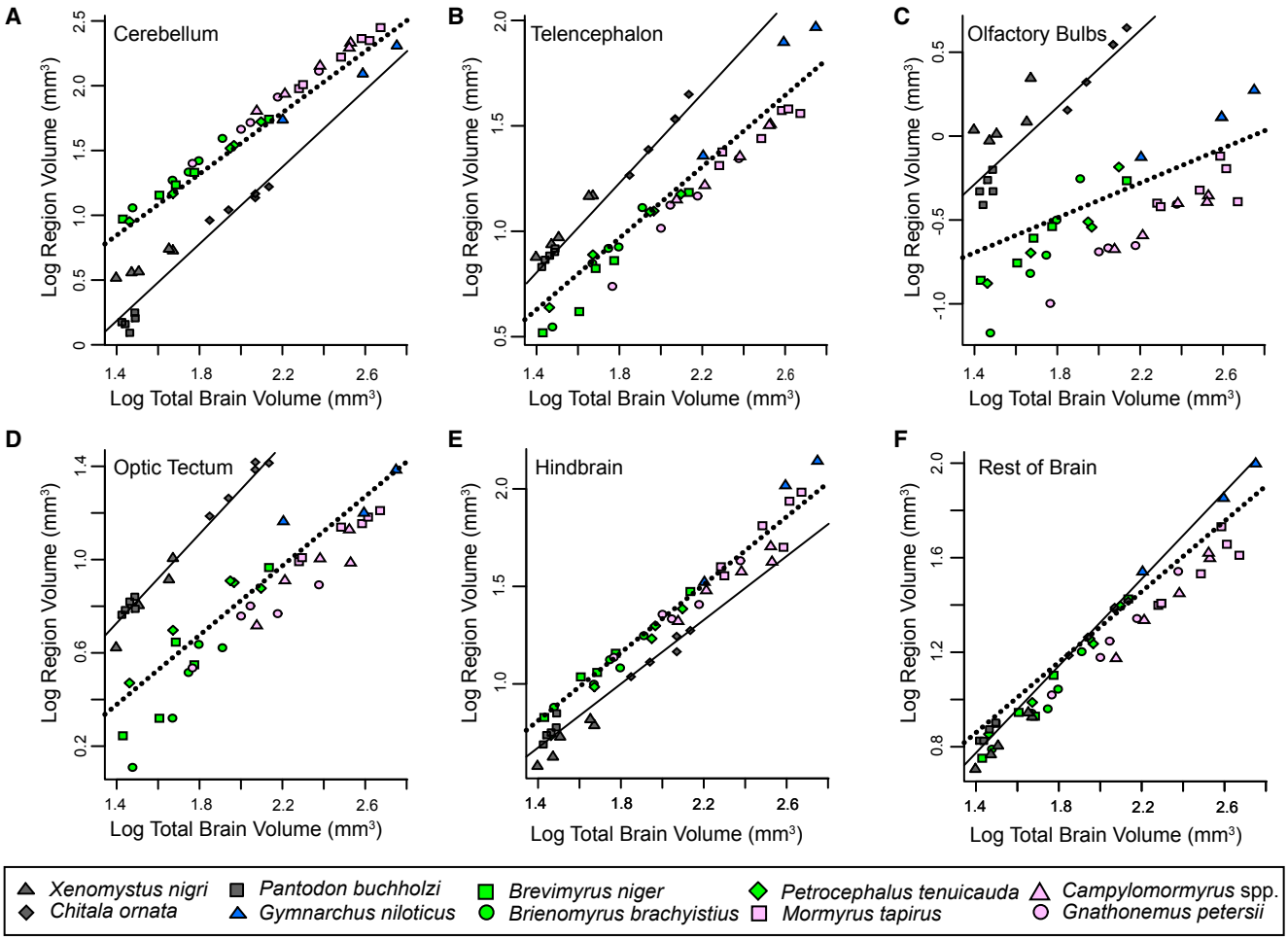

Figure 2. Mormyroids Have Enlarged Cerebellums and Hindbrains

Plots of log brain region volume (y axis) against log total brain volume (x axis) for cerebellum (A), telencephalon (B), olfactory bulbs (C), optic tectum (D), hindbrain (E), and rest of brain (F). Each point indicates a different specimen. Shapes indicate different species. Pink indicates mormyrid species with high encephalization (N = 3) (>0.2 log brain mass residuals from Sukhum et al. [11]), green indicates mormyrid species with intermediate to low encephalization (N = 3), blue indicates *G. niloticus* (N = 1), and gray indicates outgroups (N = 3). Regressions were determined using a PGLS analysis. Dotted lines show PGLS regression for mormyroids. Solid lines show PGLS for outgroups. See also Figures S1 and S2 and Table S1.

olfactory bulbs (Table S1), it is likely that this shift is largely due to variation in olfactory bulbs, which load heavily on PC2.

Shifts in Brain Shape between Mormyroids and Outgroup Species

To determine how brain shape evolved in the osteoglossomorphs, we identified landmarks and sliding semilandmarks corresponding to anatomical locations in the brains of 5 mormyrid species and 3 outgroup species (Figure 4A). Using a generalized Procrustes analysis, we scaled all brains to the same origin and volume and then performed a PCA on the landmark coordinates to characterize shape changes.

We found strong separation between mormyroids and outgroups in PC1, which explained 82.61% of variation (Figure 4B). Shape variation along PC1 primarily describes morphological changes in the cerebellum (Figure 4C). In the positive direction, the cerebellum was located in a posterior and dorsal position relative to the rest of the brain. In the negative direction, the cerebellum was expanded in every direction, leading to a more globular overall brain shape.

PC2 explained 6.73% of the variation among species, and primarily separated outgroup species *P. buchholzi* from the notopterids. These data demonstrate a dramatic shape change that occurs over the same phylogenetic timescale over which we see a mosaic enlargement of the cerebellum and hindbrain, which further emphasizes the dramatic brain region changes that occurred with the evolution of mormyroids.

DISCUSSION

We used osteoglossomorph fishes to study how brain scaling evolves in a group that also evolved a novel sensorimotor system and extreme encephalization. When looking within mormyroids or among outgroups, brain scaling generally fit the concerted model. However, a component of variation in brain region size was better explained by mosaic shifts that occurred alongside

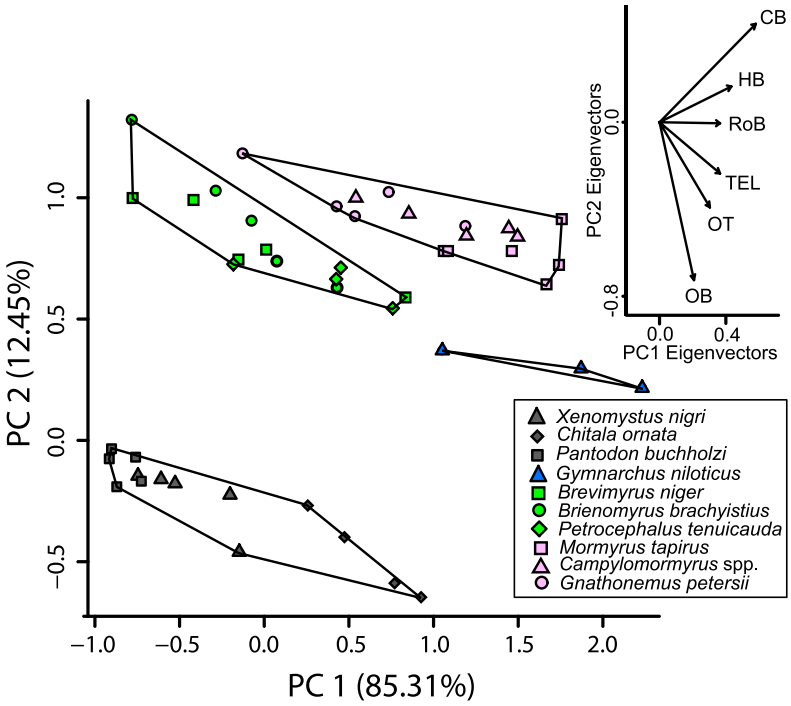

Figure 3. Mormyroids Have Distinct Brain Region Size Variation from Outgroups

Mormyroids (pink, blue, and green) segregated from outgroups (gray) in a PCA of brain region volume. The inset shows eigenvectors of brain regions for PC1 and PC2.

the evolution of active electrosensing in mormyroids. One limitation of our study is that active electrosensing evolved only once within the osteoglossomorphs. Thus, it is impossible to determine the extent to which these mosaic shifts are related to the evolution of active electrosensing as opposed to other uniquely derived traits of the mormyroids. Both the hindbrain ELL (electrosensory lateral line lobe) and cerebellum play central roles in sensorimotor integration underlying active electrosensing [17, 18]. Thus, the mosaic enlargement of these regions may have been driven partially by the evolution of active electrosensing [19]. Large portions of the cerebellum are apparently not responsive to electrosensory stimuli in *G. petersii* [19, 20]; however, an absence of response may be due to inadequate stimuli or behavioral context rather than lack of function. *G. petersii* also have an extended, flexible chin appendage that provides mechanosensory input to the cerebellum [19]. *M. tapirus* have a slightly elongated tubular snout, and *Campylomormyrus* spp. have a dramatically elongated tubular snout, but most mormyroids, including the other species we studied, lack such specializations. This suggests that the mosaic shifts characterizing mormyroids evolved before the origin of these specialized feeding adaptations. Nevertheless, it is likely that the cerebellum receives mechanosensory input and other sensory inputs across mormyrid species. It is also possible that evolutionary innovations related to learning [21, 22], complex communication [23], or other behavioral functions played a role in the extreme enlargement of the mormyroid cerebellum. Finally, an enlarged cerebellum may have been driven not by function but by constraints due to a late developmental plan shared with the ELL [24].

The telencephalon, which also receives electrosensory input [25], had a mosaic decrease in mormyroids. This decrease may reflect an artifact of using relative brain region measurements: the telencephalon could have remained the same size at the origin of mormyroids, but if other regions (i.e., cerebellum and hindbrain) experienced an independent increase in size, then the size of the telencephalon relative to the entire brain will have decreased. This may also explain the decrease in relative size of the optic tectum and olfactory bulbs in mormyroids, but these shifts may also be due to decreased reliance on visual and olfactory processing. We found no shift in the rest of the brain, which includes electrosensory midbrain but, due to limitations inherent in combining regions, we make no claims about their evolution.

Different scaling patterns could be evident at different levels of organization. Indeed, despite having a relatively small telencephalon compared to outgroups, evidence suggests that the mormyroid telencephalon is highly differentiated compared to other teleosts, as it has multiple specialized sub-regions [26]. Across songbirds, brain regions scale concertedly, but mosaic shifts are evident in the sensorimotor networks involved in learned vocal communication [27]. Fine-grained mosaic shifts are also apparent in visual nuclei of birds [28], the vagal lobe of goldfish [29], and the exterolateral nucleus of mormyrids [30]. Our study is unique because we find a number of mosaic shifts at a larger scale, across major brain regions, rather than in specific circuits. In dragon lizards, but not anolis lizards, mosaic regional shifts are related to species ecomorph [7, 8]. However, many phenotypic changes are associated with ecomorph, making it difficult to identify specific selective pressures that may have driven such shifts.

X. nigri, an outgroup species with passive electrosensing [31], has a smaller cerebellum and larger telencephalon compared to *C. ornata*. These shifts are unlike those associated with the evolution of mormyroids and therefore do not represent an intermediate phenotype. However, passive electrosensing may play qualitatively and quantitatively different roles in behavior between mormyroids and *X. nigri*, and this might drive different mosaic shifts.

To test how generalizable our findings are, and better illuminate how brain regions change with the evolution of electroreception, future studies could compare the active electrosensing gymnotiforms with their passive electrosensing relatives, the siluriforms. Qualitative descriptions of gymnotiform brains suggest potential mosaic increases in the hindbrain and midbrain compared to siluriforms [32, 33].

In mammals, evidence suggests that brain region scaling is tied to the order of regional neurogenesis [3]. Teleost fishes have indeterminate growth; adult neurogenesis occurs in every brain region [34, 35] and is prominent in the cerebellum [35, 36]. Region-specific rates of adult neurogenesis are a potential

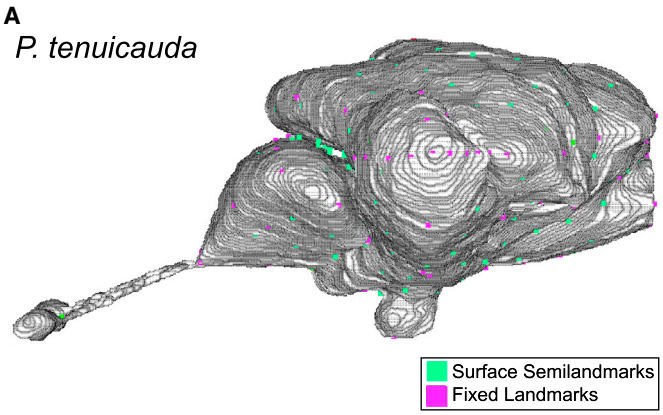

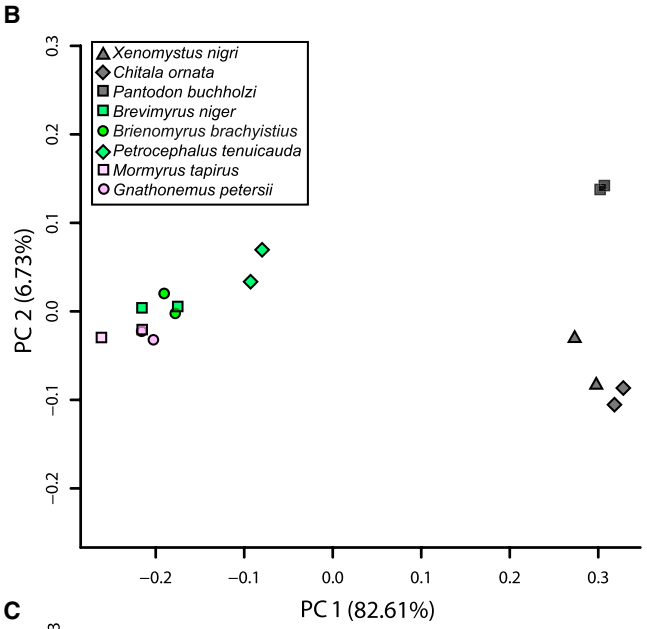

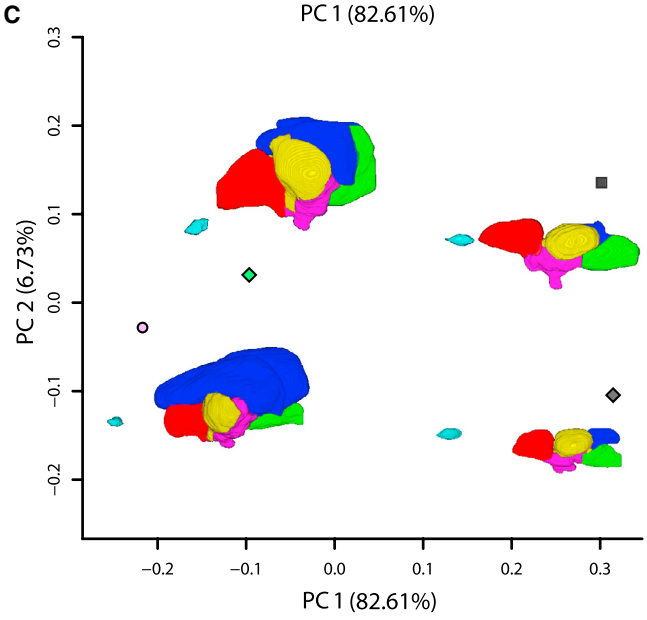

Figure 4. Mormyrids Have Distinct Brain Region Shape Variation from Outgroups

(A) Landmark template made from a 3D reconstruction of a *P. tenuicauda* brain. Magenta points indicate fixed landmarks, and green points indicate surface semilandmarks.

(B) Mormyrids (green and pink) separated from outgroups (gray) in a PCA of brain shape based on landmarks.

(C) 3D reconstructions of 4 brains illustrate brain shape differences in this PCA space.

mechanism for differential growth of brain regions between species that could underlie mosaic evolution. A study of brain development and neurogenesis in one large-brained species of mormyrid indicated several neurogenesis zones in the cerebellum that persisted throughout life [36]. Extensive adult neurogenesis may make mosaic change more easily evolved in teleost fish than in mammals. Chondrichthyans also have persistent neurogenesis in the cerebellum [37], but there is no evidence for mosaic shifts [6]. Based on these studies, we speculate that adult neurogenesis may be permissive for mosaic shifts, and a strong selective force is needed to act on that latent potential to drive mosaic change. In mormyrids, dramatic regional changes evolved alongside the evolution of a novel sensorimotor system. Our results support major aspects of both the concerted and mosaic hypotheses and suggest that concerted evolution is prevalent even with dramatic changes in total brain size but that mosaic shifts can occur when behavioral novelty evolves.

STAR★METHODS

Detailed methods are provided in the online version of this paper and include the following:

- KEY RESOURCES TABLE
- CONTACT FOR REAGENT AND RESOURCE SHARING
- EXPERIMENTAL MODEL AND SUBJECT DETAILS
  - Specimens
- METHOD DETAILS
  - Perfusion
  - Micro-computed tomography scans
- QUANTIFICATION AND STATISTICAL ANALYSIS
  - Brain Organization and Structural Delineation
  - Determining brain volumes
  - Phylogenetic comparisons
  - Geometric morphometric analysis of brain shape

SUPPLEMENTAL INFORMATION

Supplemental Information includes three figures, two tables, and one video and can be found with this article online at https://doi.org/10.1016/j.cub.2018.10.038.

ACKNOWLEDGMENTS

We thank M. Kawasaki for providing *G. niloticus* specimens, and M. Silva and D. Leib for assistance with microCT scans. This work was funded by NSF IOS 1255396.

AUTHOR CONTRIBUTIONS

Conceptualization & Methodology, K.V.S. and B.A.C.; Investigation & Formal Analyses, K.V.S. and J.S.; Writing – Original Draft, K.V.S.; Writing – Review & Editing, B.A.C. and K.V.S.

DECLARATION OF INTERESTS

The authors declare no competing interests.

Received: May 22, 2018
Revised: September 26, 2018
Accepted: October 15, 2018
Published: November 15, 2018

REFERENCES

1. Nieuwenhuys, R., Donkelaar, H.J.T., and Nicholson, C. (1998). The Central Nervous System of Vertebrates (Springer-Verlag).
2. Striedter, G.F. (2005). Principles of Brain Evolution (Sinauer Associates).
3. Barton, R.A., and Harvey, P.H. (2000). Mosaic evolution of brain structure in mammals. Nature *405*, 1055–1058.
4. Finlay, B.L., and Darlington, R.B. (1995). Linked regularities in the development and evolution of mammalian brains. Science *268*, 1578–1584.
5. Charvet, C.J., and Striedter, G.F. (2009). Developmental origins of mosaic brain evolution: morphometric analysis of the developing zebra finch brain. J. Comp. Neurol. *514*, 203–213.
6. Yopak, K.E., Lisney, T.J., Darlington, R.B., Collin, S.P., Montgomery, J.C., and Finlay, B.L. (2010). A conserved pattern of brain scaling from sharks to primates. Proc. Natl. Acad. Sci. USA *107*, 12946–12951.
7. Powell, B.J., and Leal, M. (2012). Brain evolution across the Puerto Rican anole radiation. Brain Behav. Evol. *80*, 170–180.
8. Hoops, D., Vidal-García, M., Ullmann, J.F.P., Janke, A.L., Stait-Gardner, T., Duchêne, D.A., Price, W.S., Whiting, M.J., and Keogh, J.S. (2017). Evidence for concerted and mosaic brain evolution in dragon lizards. Brain Behav. Evol. *90*, 211–223.
9. Hager, R., Lu, L., Rosen, G.D., and Williams, R.W. (2012). Genetic architecture supports mosaic brain evolution and independent brain-body size regulation. Nat. Commun. *3*, 1079.
10. Sayol, F., Lefebvre, L., and Sol, D. (2016). Relative brain size and its relation with the associative pallium in birds. Brain Behav. Evol. *87*, 69–77.
11. Sukhum, K.V., Freiler, M.K., Wang, R., and Carlson, B.A. (2016). The costs of a big brain: extreme encephalization results in higher energetic demand and reduced hypoxia tolerance in weakly electric African fishes. Proc. Biol. Sci. *283*, 20162157.
12. Butler, A.B., and Hodos, W. (2005). Comparative Vertebrate Neuroanatomy: Evolution and Adaptation (Wiley-Interscience).
13. Carlson, B.A., and Arnegard, M.E. (2011). Neural innovations and the diversification of African weakly electric fishes. Commun. Integr. Biol. *4*, 720–725.
14. Sullivan, J.P., Lavoué, S., and Hopkins, C.D. (2000). Molecular systematics of the African electric fishes (Mormyroidea: Teleostei) and a model for the evolution of their electric organs. J. Exp. Biol. *203*, 665–683.
15. Lavoué, S., Sullivan, J.P., and Hopkins, C.D. (2003). Phylogenetic utility of the first two introns of the S7 ribosomal protein gene in African electric fishes (Mormyroidea: Teleostei) and congruence with other molecular markers. Biol. J. Linn. Soc. Lond. *78*, 273–292.
16. Lavoué, S., and Sullivan, J.P. (2004). Simultaneous analysis of five molecular markers provides a well-supported phylogenetic hypothesis for the living bony-tongue fishes (Osteoglossomorpha: Teleostei). Mol. Phylogenet. Evol. *33*, 171–185.
17. Bell, C.C., and Szabo, T. (1986). Electroreception in mormyrid fish: central anatomy. In Electroreception, T.H. Bullock, and W. Heiligenberg, eds. (John Wiley & Sons), pp. 375–421.
18. Bell, C.C. (1986). Electroreception in mormyrid fish: central physiology. In Electroreception, T.H. Bullock, and W. Heiligenberg, eds. (John Wiley and Sons), pp. 423–452.
19. Russell, C.J., and Bell, C.C. (1978). Neuronal responses to electrosensory input in mormyrid valvula cerebelli. J. Neurophysiol. *41*, 1495–1510.
20. Finger, T.E., Bell, C.C., and Russell, C.J. (1981). Electrosensory pathways to the valvula cerebelli in mormyrid fish. Exp. Brain Res. *42*, 23–33.
21. von der Emde, G. (1990). Discrimination of objects through electrolocation in the weakly electric fish, *Gnathonemus petersii*. J. Comp. Physiol. A Neuroethol. Sens. Neural Behav. Physiol. *167*, 413–421.
22. Emde, G., and Bleckmann, H. (1998). Finding food: senses involved in foraging for insect larvae in the electric fish *Gnathonemus petersii*. J. Exp. Biol. *201*, 969–980.

23. Wong, R.Y., and Hopkins, C.D. (2007). Electrical and behavioral courtship displays in the mormyrid fish *Brienomyrus brachyistius*. J. Exp. Biol. *210*, 2244–2252.
24. Montgomery, J., and Bodznick, D. (2017). From Cerebellum-like to Cerebellum: Evolution by Duplication? (Oxford University Press).
25. Prechtl, J.C., von der Emde, G., Wolfart, J., Karamürsel, S., Akoev, G.N., Andrianov, Y.N., and Bullock, T.H. (1998). Sensory processing in the pallium of a mormyrid fish. J. Neurosci. *18*, 7381–7393.
26. Meek, J., Joosten, H.W.J., and Steinbusch, H.W.M. (1989). Distribution of dopamine immunoreactivity in the brain of the mormyrid teleost *Gnathonemus petersii*. J. Comp. Neurol. *281*, 362–383.
27. Moore, J.M., and DeVoogd, T.J. (2017). Concerted and mosaic evolution of functional modules in songbird brains. Proc. Biol. Sci. *284*, 20170469.
28. Gutiérrez-Ibáñez, C., Iwaniuk, A.N., Moore, B.A., Fernández-Juricic, E., Corfield, J.R., Krilow, J.M., Kolominsky, J., and Wylie, D.R. (2014). Mosaic and concerted evolution in the visual system of birds. PLoS ONE *9*, e90102.
29. Morita, Y., and Finger, T.E. (1985). Topographic and laminar organization of the vagal gustatory system in the goldfish, *Carassius auratus*. J. Comp. Neurol. *238*, 187–201.
30. Carlson, B.A., Hasan, S.M., Hollmann, M., Miller, D.B., Harmon, L.J., and Arnegard, M.E. (2011). Brain evolution triggers increased diversification of electric fishes. Science *332*, 583–586.
31. Bullock, T.H., and Northcutt, R.G. (1982). A new electroreceptive teleost: *Xenomystus nigri* (Osteoglossiformes: Notopteridae). J. Comp. Physiol. *148*, 345–352.
32. Albert, J.S. (2001). Species Diversity and Phylogenetic Systematics of America Knifefishes (Gymnotiformes, Teleostei) (University of Michigan).
33. Abrahao, V.P., Pupo, F.M., and Shibatta, O.A. (2018). Comparative brain gross morphology of the Neotropical catfish family Pseudopimelodidae (Osteichthyes, Ostariophysi, Siluriformes), with phylogenetic implications. Zool. J. Linn. Soc. *184*, 750–772.
34. Kaslin, J., Ganz, J., and Brand, M. (2008). Proliferation, neurogenesis and regeneration in the non-mammalian vertebrate brain. Philos. Trans. R. Soc. Lond. B Biol. Sci. *363*, 101–122.
35. Zupanc, G.K. (2006). Neurogenesis and neuronal regeneration in the adult fish brain. J. Comp. Physiol. A Neuroethol. Sens. Neural Behav. Physiol. *192*, 649–670.
36. Radmilovich, M., Barreiro, I., Iribarne, L., Grant, K., Kirschbaum, F., and Castelló, M.E. (2016). Post-hatching brain morphogenesis and cell proliferation in the pulse-type mormyrid *Mormyrus rume proboscirostris*. J. Physiol. Paris *110*, 245–258.
37. Rodríguez-Moldes, I., Ferreiro-Galve, S., Carrera, I., Sueiro, C., Candal, E., Mazan, S., and Anadón, R. (2008). Development of the cerebellar body in sharks: spatiotemporal relations of Pax6 expression, cell proliferation and differentiation. Neurosci. Lett. *432*, 105–110.
38. Merzin, M. (2008). Applying stereological method in radiology. Volume measurement. Bachelor's thesis (University of Tartu).
39. Tamura, K., Peterson, D., Peterson, N., Stecher, G., Nei, M., and Kumar, S. (2011). MEGA5: molecular evolutionary genetics analysis using maximum likelihood, evolutionary distance, and maximum parsimony methods. Mol. Biol. Evol. *28*, 2731–2739.
40. R Core Team (2012). R: a language and environment for statistical computing (R Foundation for Statistical Computing).
41. Schindelin, J., Arganda-Carreras, I., Frise, E., Kaynig, V., Longair, M., Pietzsch, T., Preibisch, S., Rueden, C., Saalfeld, S., Schmid, B., et al. (2012). Fiji: an open-source platform for biological-image analysis. Nat. Methods *9*, 676–682.
42. Schneider, C.A., Rasband, W.S., and Eliceiri, K.W. (2012). NIH Image to ImageJ: 25 years of image analysis. Nat. Methods *9*, 671–675.
43. Herculano-Houzel, S., Manger, P.R., and Kaas, J.H. (2014). Brain scaling in mammalian evolution as a consequence of concerted and mosaic changes in numbers of neurons and average neuronal cell size. Front. Neuroanat. *8*, 77.
44. Azevedo, F.A.C., Carvalho, L.R., Grinberg, L.T., Farfel, J.M., Ferretti, R.E., Leite, R.E., Jacob Filho, W., Lent, R., and Herculano-Houzel, S. (2009). Equal numbers of neuronal and nonneuronal cells make the human brain an isometrically scaled-up primate brain. J. Comp. Neurol. *513*, 532–541.
45. Bandeira, F., Lent, R., and Herculano-Houzel, S. (2009). Changing numbers of neuronal and non-neuronal cells underlie postnatal brain growth in the rat. Proc. Natl. Acad. Sci. USA *106*, 14108–14113.
46. Roberts, N., Puddephat, M.J., and McNulty, V. (2000). The benefit of stereology for quantitative radiology. Br. J. Radiol. *73*, 679–697.
47. Ives, A.R., Midford, P.E., and Garland, T., Jr. (2007). Within-species variation and measurement error in phylogenetic comparative methods. Syst. Biol. *56*, 252–270.
48. Orme, D. (2012). Caper: comparative analyses of phylogenetics and evolution in R. R package version 0.5. https://CRAN.R-project.org/package=caper.
49. Pinheiro, J., Bates, D., DebRoy, S., and Sarkar, D.; R Core Team. (2015). nlme: linear and nonlinear mixed effects models. R package version 3.1-120. https://CRAN.R-project.org/package=nlme.
50. Paradis, E., Claude, J., and Strimmer, K. (2004). APE: analyses of phylogenetics and evolution in R language. Bioinformatics *20*, 289–290.
51. Revell, L.J. (2012). phytools: an R package of phylogenetic comparative biology (and other things). Methods Ecol. Evol. *3*, 217–223.
52. Adams, D.C., Collyer, M.L., Kaliontzopoulou, A., and Sherratt, E. (2017). Geomorph: software for geometric morphometric analyses. R package version 3.0.5. https://cran.r-project.org/package=geomorph.

STAR★METHODS

KEY RESOURCES TABLE

REAGENT or RESOURCE	SOURCE	IDENTIFIER
Chemicals, Peptides, and Recombinant Proteins		
Tricaine methanesulfonate (MS-222)	Western Chemical Inc	NC0242409; CAS: 886-86-2
Paraformaldehyde	Sigma-Aldrich	P6148; CAS: 30525-89-4
Phosphomolybdic acid hydrate (PMA)	Fisher Scientific Company	AC417890250; CAS: 51429-74-4
Experimental Models: Organisms/Strains		
Pantodon buchholzi	Bailey's Tropical Fish	N/A
Chitala ornata	Bailey's Tropical Fish	N/A
Xenomystus nigri	Bailey's Tropical Fish	N/A
Gymnarchus niloticus	Dr. Masashi Kawasaki	N/A
Campylomormyrus spp.	Bailey's Tropical Fish	N/A
Gnathonemus petersii	Bailey's Tropical Fish	N/A
Mormyrus tapirus	Bailey's Tropical Fish	N/A
Brevimyrus niger	Bailey's Tropical Fish	N/A
Petrocephalus tenuicauda	Bailey's Tropical Fish	N/A
Brienomyrus brachyistius	Bailey's Tropical Fish	N/A
Software and Algorithms		
Volumest	[38]	20101017.jar; http://lepo.it.da.ut.ee/~markkom/volumest/
MEGA v. 5.1	[39]	https://www.megasoftware.net/
R v 3.5.0	[40]	https://www.r-project.org/
FIJI	[41, 42]	https://fiji.sc/

CONTACT FOR REAGENT AND RESOURCE SHARING

Further information and requests for resources and reagents should be directed to and will be fulfilled by the Lead Contact, Bruce A. Carlson (carlson.bruce@wustl.edu).

EXPERIMENTAL MODEL AND SUBJECT DETAILS

Specimens

We measured brains of 49 specimens from 6 Mormyridae species, 2 Notopteridae species, and 1 Pantodon species, and 3 specimens of the only known Gymnarchidae species. All Mormyridae, Notopteridae, and Pantodon were obtained through the aquarium trade and kept in lab conditions of 12:12 light:dark cycle with water temperature of 25-29°C. Formalin-fixed Gymnarchidae specimens were provided by Dr. Masashi Kawasaki. All procedures were in accordance with guidelines established by the National Institutes of Health and were approved by the Animal Care and Use Committee at Washington University in St. Louis.

METHOD DETAILS

Perfusion

Fish were anesthetized with a 300 mg/mL solution of tricaine methanesulfonate (MS-222) and then perfused transcardially with heparinized Hickman's Ringer solution, followed by 4% buffered paraformaldehyde. All specimens were decapitated and set in 4% paraformaldehyde at 4°C overnight. Specimens were then transferred to 0.1 M phosphate buffer (PB). Large- and small-brained species were stained in 10% and 5% phosphomolybdic acid (PMA) respectively for 1 week and then transferred to 0.1M PB.

Micro-computed tomography scans

Micro-computed tomography (microCT) scans were done in the Musculoskeletal Research Center at the Barnes-Jewish Research Institute using a MicroCT scanner (SCANCO uCT40 Medical model 10 version SCANO_V1.2a). Scans were done at 55kV energy/intensity, 300 ms exposure time, 22 μA exposure amperage. Slice thickness was set at 0.01 mm. Specimens were

held in place in scan tubes with a 20% agar solution. Tubes used had 20mm or 30mm scanning diameters depending on the size of the specimen.

QUANTIFICATION AND STATISTICAL ANALYSIS

Brain Organization and Structural Delineation

We measured 6 distinct regions of the brain and used a series of consistent landmarks and planes to identify the various regions (Figure S3).

The horizontal plane (Figures S3A, S3C, and S3E, light green plane) divided the brain into dorsal and ventral areas and was 90° to the midline of the brain. In non-mormyroids, the horizontal plane ran from the point of the telencephalon (TEL) that was furthest ventral in a straight plane back to the furthest dorsal part of the spinal cord (Figure S3E, landmark a). In mormyroids, the cerebellum (CB) has pushed the rest of the brain further ventral, so to mark the same separation as in the non-mormyroids, the horizontal plane ran from the point of the telencephalon that was furthest dorsal in a straight plane back to the furthest dorsal bulge of the hindbrain (Figures S3A and S3C, landmark a) that did not include the electrosensory lateral line lobe (ELL) (Figures S3A and S3C, landmark b).

Olfactory bulb (OB) was an ellipsoid bulb at the anterior end of the skull cavity. It was connected to the rest of the brain by the olfactory tract but was otherwise clearly separate from the rest of the brain (Figure 1B).

Telencephalon (TEL) was the ellipsoid shaped bulb in the most anterior area of the brain. In all species, the caudal end of the telencephalon was determined by the telencephalon plane (Figures S3A, S3C, and S3E, red plane) which was a transverse plane 90° from the horizontal plane and was marked by the furthest posterior bulge of the telencephalon (Figures S3A, S3C, and S3E, landmark c).

Optic tectum (OT) was the furthest lateral and anterior region in the midbrain. The optic tectum forms a cup-like shape that encircles the rest of the midbrain. The furthest anterior area was marked by the telencephalon plane (Figures S3A, S3C, and S3E, red plane). The most posterior end of the optic tectum is marked by 3 planes. One is the optic tectum plane (Figure S3, yellow plane), which connects medial-laterally the furthest posterior curves of the torus semicircularis (Figures S3B, S3D, and S3F, landmark d). The other posterior ends of the optic tectum are marked by the lateral optic tectum planes (Figures S3B, S3D, and S3F, orange planes), which connected the end of the optic tectum plane to the most lateral curve of the torus semicircularis. In non-mormyroids, this demarcation consists of two planes due to the optic tectum wrapping tighter around the torus semicircularis (Figure S3F, landmark d). The furthest medial regions were determined by the optic tectum medial planes (Figures S3B, S3D, and S3F, dark green plane). These were marked by the furthest lateral curve of the thalamus (Figures S3B, S3D, and S3F, landmark e).

Hindbrain (HB) was separated from spinal cord by the hindbrain plane (Figures S3A, S3C, and S3E, dark blue plane), which was a transverse plane 90° from the midbrain plane, and which marked the furthest posterior point of the cerebellum, ELL (Figures S3A and S3C, landmark b), or hindbrain dorsal bulge (Figures S3A, S3C, and S3E, landmark a), whichever was furthest posterior. ELL is only clearly identifiable in our mormyroid species and was included in the hindbrain region. Hindbrain included everything posterior to the anterior-hindbrain plane (Figures S3A, S3C, and S3E, purple plane). In outgroup species, the anterior-hindbrain plane runs at approximately a 45° angle from horizontal plane from the hindbrain dorsal bulge (Figure S3C, landmark a) to the concave curve of the hindbrain (Figure S3C, landmark g). In mormyrids, the anterior-hindbrain plane runs from the outward bulge of the lobus caudalis cerebelli (Figures S3A and S3C, landmark f) to the concave curve of the hindbrain (Figures S3A and S3C, landmark g). The cerebellum could engulf the hindbrain both dorsally and laterally. We used the dorsal-hindbrain plane to mark the furthest most dorsal curve of the hindbrain (Figures S3A, S3C, and S3E, white plane). The lateral-hindbrain planes (Figures S3B, S3D, and S3F, light blue plane) marked the furthest anterior-medial point of the convex curve of the cerebellum (Figures S3B and S3D, landmark h) to the furthest posterior curve of the ELL (Figures S3B and S3D, landmark i).

In non-mormyroid species, the cerebellum (CB) was a small ellipsoid at the farthest dorsal, posterior end of the brain. In mormyroids, the cerebellum was a helmet shaped area that was most of the dorsal area of the brain. The most ventral end of the cerebellum was marked by the horizontal plane.

All other parts of the brain, including the torus semicircularis, hypothalamus, and thalamus were defined as rest of brain (RoB). There is large variation in the size and shape of the rest of brain region across the osteoglossomorphs due to the expansion of the cerebellum pushing the midbrain region further ventral (Figure 1) [26]. Thus, it was not possible to reliably and objectively define landmarks to separate hypothalamus, thalamus, or midbrain regions across species. Previous studies have similarly combined small, distinct brain regions into a rest-of-brain region for comparison with other brain regions [43–45].

Determining brain volumes

The order in which specimens were measured was randomized. We used the ImageJ plugin Volumest to determine brain region volume [38]. Brain region area was manually traced every 2-10 slices, where slices were 10 μm thick with a grid thickness of 0.1mm. Because brain regions varied greatly in size, we used more precise methods for smaller regions. If a brain region was greater than $4mm^3$, we measured the area of the region every 10 slices. If a brain region was smaller than $4mm^3$ but larger than $1mm^3$, we measured the area of the region every 5 slices instead of 10. If the region was smaller than $1mm^3$, we measured the region every 2 slices instead of 10 and magnified it in size 2X. Volumest then used stereological methods to estimate volume of each region [46].

After 15 specimens were measured, 3 of those specimens were selected to be re-measured twice, blind to the previous results. We calculated the coefficient of variation (CV) of each region using the 3 volume measurements. The CVs for each re-measurement were below 3%, indicating high precision in volume measurements (Table S2).

Phylogenetic comparisons

We used a bootstrapped maximum-likelihood tree from 73 Cytb osteoglossomorph sequences built in MEGA v. 5.1 [39]. To include data from species that have not been sequenced, we used sequence data from within monophyletic genera and chose the species sequence with the shortest phylogenetic distance from the genus node. We pruned lineages for which we did not have brain region measurements. To account for the effects of phylogeny, we used a version of phylogenetic generalized least-squares (PGLS) which accounts for intraspecific variation [47]. To determine whether a grade shift had occurred, we created a PGLS fit for each grade, and then compared those PGLS relationships using an analysis of covariance (ANCOVA) (Table S2).

To incorporate phylogeny in a principal component analysis (PCA), we performed a phylogenetic PCA on species means, then used the rotation obtained from this PCA to compute scores for individual specimens. All phylogenetic analyses were performed in R using the phytools, ape, caper and nlme packages [40, 48–51].

Geometric morphometric analysis of brain shape

We analyzed 2 specimens each from 5 mormyrid and 3 outgroup species. We did not include *Campylomormyus* spp. because of their phenotypic and phylogenetic similarity to *G. petersii*, and we did not include *G. niloticus* because they were fixed by immersion in formalin instead of with a perfusion of paraformaldehyde, which may result in shape differences unrelated to natural variation. We used geometric morphometric analysis to quantify shape variation using homologous landmarks, while controlling for brain size. First, we constructed three-dimensional models of the brains by segmenting brain from non-brain in each microCT scan image using a segmentation editor program in FIJI and reconstructing those segments into 3D surface images of the brain [41, 42].

Next, we created a brain template. The template defined the landmark coordinates across all of the brains, and shape variation analysis took into account changes in these coordinates. We used *Petrocephalus tenuicauda* to create a template to define 418 landmarks across the surface of the brains. We determined 98 fixed landmarks based on anatomically-defined locations. We then defined 66 of these points as sliding curve semilandmarks, which would take into account the shape of curves in the brain regions. We placed the 98 fixed landmarks on each brain utilized in the analysis so that the template could be applied based on their locations. Using k-means clustering, we also included 320 sliding surface semilandmark points, which would allow us to analyze the variation across the entire brain surface in areas beyond the fixed landmarks. A k-means clustering algorithm evenly spaced these points across the surface of the brain. K centroids were first estimated in the coordinates of the brain surface, and then each data point in the surface was assigned to the nearest centroid. This creates 320 clusters, where a number of data points were associated with each of the 320 centroids. Clusters were determined by the minimal sum of the distances between each assigned data point and the centroid. This step was performed again by averaging the coordinates of all the data points assigned to a cluster – the mean of those coordinates becomes that cluster's centroid for the next iteration. We performed 100 iterations until data points no longer moved to other clusters, or the sum of the distances reached a minimum value. The coordinates of the centroids of each of the 320 clusters were assigned to surface semilandmarks, for a total of 320 surface semilandmarks that were then added to the template. We eliminated any non-shape variation by performing a generalized Procrustes analysis of the raw coordinate data, which translates, scales, and rotates all specimen landmark coordinates so that all landmarks are oriented similarly between brains. We performed a PCA using all the aligned landmarks. All analyses were done using geomorph in R [52].

Current Biology, Volume *28*

Supplemental Information

Extreme Enlargement of the Cerebellum in a Clade of Teleost Fishes that Evolved a Novel Active Sensory System

Kimberley V. Sukhum, Jerry Shen, and Bruce A. Carlson

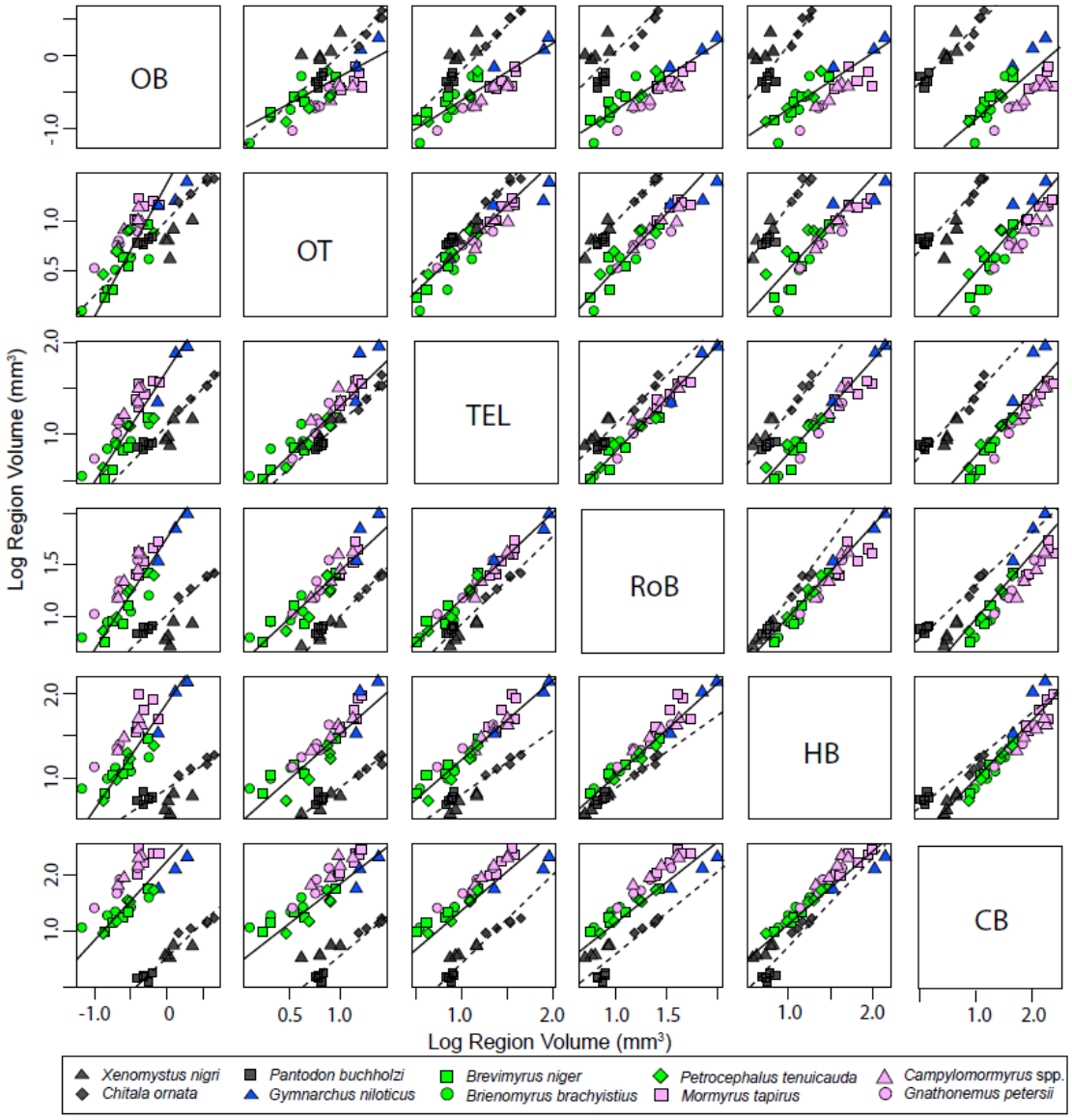

Figure S1. Grade shift evident between mormyroid and outgroup species in most region by region comparisons, Related to Figure 2.

Matrix of scatterplots of log brain region volume against log brain region volume for olfactory bulbs, optic tectum, telencephalon, rest of brain, hindbrain, and cerebellum. Y-intercepts vary depending on grade. Each point indicates a different specimen. Shapes indicate different species. Pink points indicate mormyrid species with high encephalization (N=3) (>0.2 log brain mass residuals from Sukhum et al. [S1]), green points indicate the rest of the mormyrid species with intermediate to small encephalization (N=3), blue points indicate sister taxon to mormyrids, *G. niloticus* (N=1), and grey points indicate outgroup species (N=3). Regressions were determined using a PGLS analysis that incorporated intraspecific variation. Solid line shows PGLS regression for mormyroid species. Dashed line shows PGLS for outgroup species.

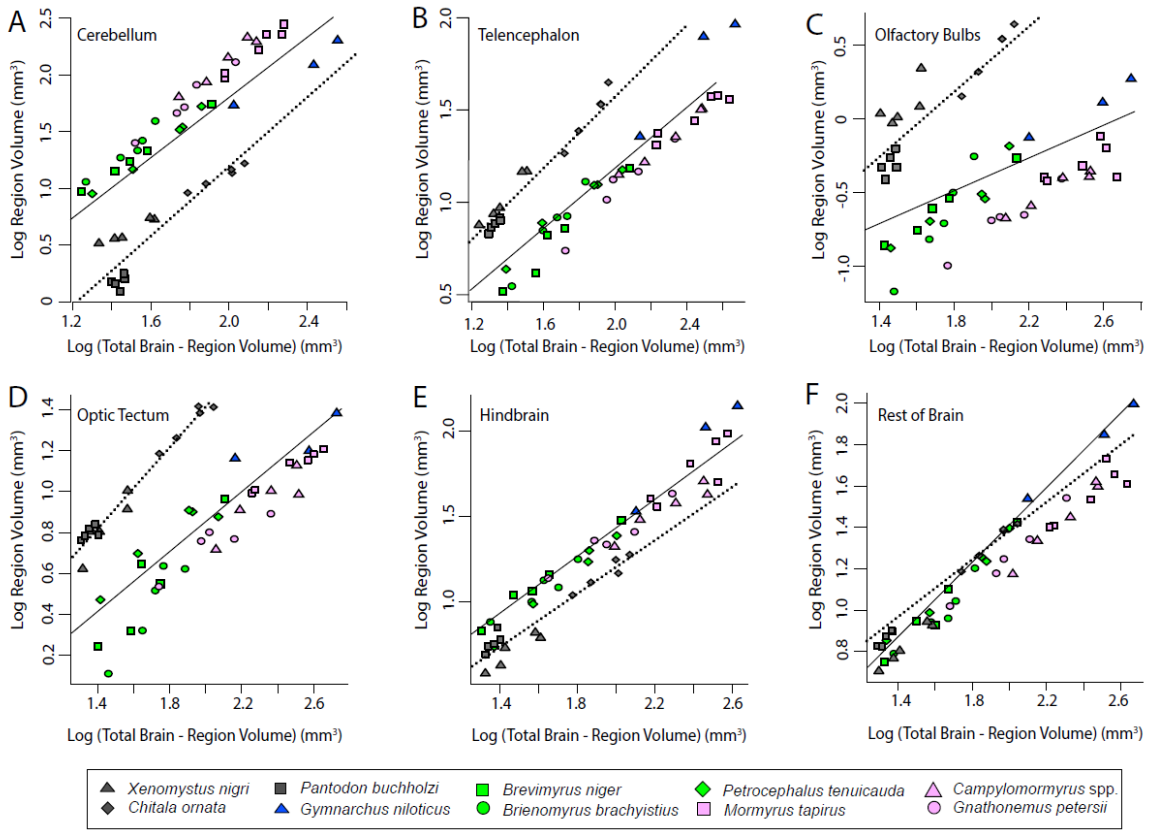

Figure S2. Grade shift evident between mormyroid and outgroup species in cerebellum, telencephalon, olfactory bulbs, optic tectum, hindbrain, and rest of brain regions, Related to Figure 2.

(A-F) Plots of log brain region volume (y-axis) against log total brain volume – region volume (x-axis) for cerebellum (A), telencephalon (B), olfactory bulbs (C), optic tectum (D), hindbrain (E), and rest of brain (F). Y-intercepts vary depending on grade. Each point indicates a different specimen. Shapes indicate different species. Pink points indicate mormyrid species with high encephalization (N=3) (>0.2 log brain mass residuals from Sukhum et al. [S1]), green points indicate the rest of the mormyrid species with intermediate to small encephalization (N=3), blue points indicate sister taxon to mormyrids, *G. niloticus* (N=1), and grey points indicate outgroup species (N=3). Regressions were determined using a PGLS analysis that incorporated intraspecific variation. Solid line shows PGLS regression for mormyroid species. Dashed line shows PGLS for outgroup species.

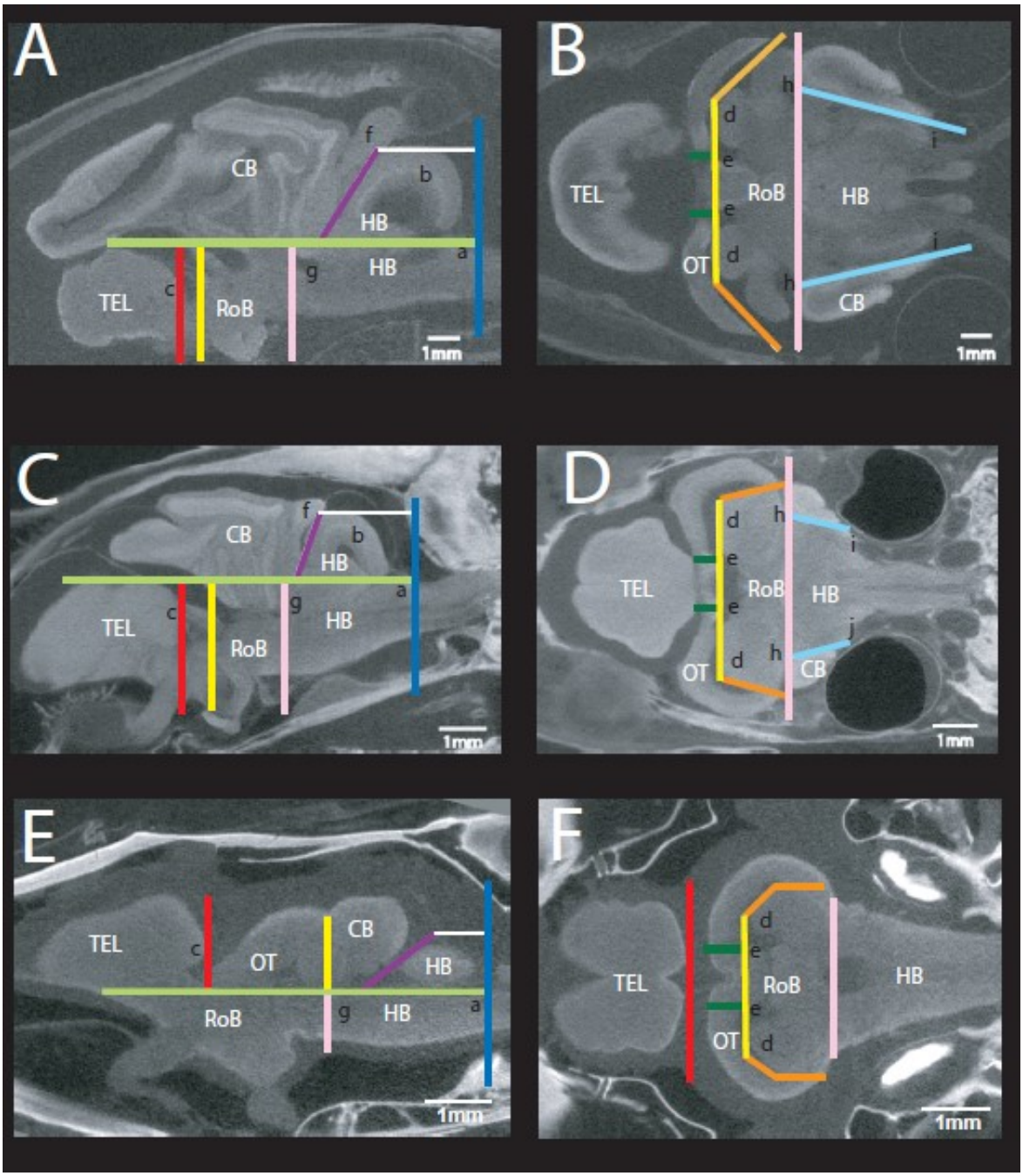

Figure S3. Telencephalon (TEL), cerebellum (CB), optic tectum (OT), olfactory bulb (OB), and rest of brain (RoB) regions were determined using consistent landmarks and planes across all species, Related to STAR Methods.

Brain regions were determined using landmarks and planes. Example brain slices from *Gnathonemus petersii* (A,B), *Petrocephalus tenuicauda* (C,D), and *Pantodon buchholzi* (E,F) indicate positioning of the landmarks (letters) and planes (lines). Images were made by averaging ten 10 μm slices (100 μm total width) from a sagittal plane of the brain (A,C,E) or a horizontal plane of the brain (B,D,F). Brains were oriented in a sagittal plane with posterior to the right and dorsal on top (A,C,E) or a horizontal plane with posterior to the right (B,D,F).

	Outgroups vs Mormyroid Species		Large vs Small and Intermediate Brained Mormyrid Species		*X. nigri* vs *C. ornata*	
Region	Slope	Intercept	Slope	Intercept	Slope	Intercept
CB	0.355	**$<10^{-12}$**	0.444	0.271	0.834	**<0.05**
TEL	0.648	**$<10^{-6}$**	0.818	0.2901	0.141	**<10^-4**
OT	0.235	**$<10^{-13}$**	0.104	0.392	0.241	0.722
OB	0.236	**$<10^{-8}$**	0.942	**$<10^{-4}$**	0.104	0.064
RoB	0.651	0.217	0.170	0.7137	0.829	**$<10^{-5}$**
AHB	0.619	**<0.01**	0.600	0.7077	0.900	0.141

Table S1. Analysis of covariance (ANCOVA) p-values for slope and intercept for each brain region, Related to Figure 2.
ANCOVAs were performed for different grade comparisons.

Species	**OB (%)**	**TEL (%)**	**OT (%)**	**RoB (%)**	**AHB (%)**	**CB (%)**	**Total Vol (%)**
B. brachyistius	0.972	0.838	1.375	1.089	0.078	0.868	0.485
B. niger	2.602	0.149	0.663	0.715	1.401	1.484	0.225
C. ornata	1.856	0.710	0.284	1.537	0.779	0.673	0.686
P. buchholzi	0.603	1.624	2.057	1.251	0.478	1.058	1.185
G. petersii	1.246	0.255	0.673	1.031	1.010	0.300	0.377
P. tenuicauda	0.448	0.334	0.809	0.278	1.129	0.472	0.407
Campylomormyrus spp.	1.970	0.514	1.045	1.773	0.777	0.370	0.602
M. tapirus	1.029	2.285	0.948	1.173	0.393	0.637	0.519
Campylomormyrus spp.	2.044	1.296	1.981	0.430	1.187	0.401	0.535
B. brachyistius	1.852	1.440	1.207	0.954	0.487	0.619	0.543

Table S2. Coefficient of variation (CV), expressed as a percentage, of three repeated volume measurements for each region for 10 different osteoglossomorph specimens, Related to STAR Methods.

Supplemental References

[S1] Sukhum KV, Freiler MK, Wang R, Carlson BA (2016) The costs of a big brain: extreme encephalization results in higher energetic demand and reducded hypoxia tolerance in weakly electric African fishes *Proc. Royal Soc. Lond B* 283.